Mineral fibres and environmental monitoring: A comparison of different analytical strategies in New Caledonia

Mineral fibres and environmental monitoring: a comparison of different analytical strategies in New Caledonia.

Jasmine Rita Petriglieri[a, b, *], Christine Laporte-Magoni[a], Peggy Gunkel-Grillon[a], Mario Tribaudino[b], Danilo Bersani[c], Orietta Sala[d], Monika Le Mestre[a], Ruggero Vigliaturo[e], Nicola Bursi Gandolfi[f], Emma Salvioli-Mariani[b].

[a] Institute of Exact and Applied Sciences, Université de la Nouvelle Calédonie, Campus de Nouville - BP R4 - 98851 Nouméa Cedex, New Caledonia, France.

[b] Department of Chemistry, Life Sciences and Environmental Sustainability, University of Parma, Parco Area delle Scienze 157/A, I-43124 Parma, Italy.

[c] Department of Mathematical, Physical and Computer Sciences, University of Parma, Parco Area delle Scienze 7/A, I-43124 Parma, Italy.

[d] Arpae Emilia Romagna, Sezione Provinciale di Reggio Emilia - Centro Regionale Amianto - Via Amendola 2, I-42122, Reggio Emilia, Italy. Presently retired.

[e] Department of Earth and Environmental Science, University of Pennsylvania, 240 S. 33rd Street, Hayden Hall, Philadelphia, PA 19104-6316, U.S.A.

[f] Department of Chemical and Geological Sciences, University of Modena and Reggio Emilia, Via Università 4, I-41125, Modena, Italy.

* Corresponding author.

Abstract

Covered by ultrabasic units for more than a third of its surface, the New Caledonia (South West Pacific) is one of the largest world producers of Ni-ore from lateritic deposits. Almost all outcrops of geological units and open mines contain serpentine and amphibole, also as asbestos varieties. In this geological context, in which weathering processes had a great contribution in the production and dispersion of mineral fibres into the environment, the development of a routinely analytical strategy, able to discriminate an asbestiform fibre from a non-harmful particle, is a pivotal requisite. However, the acquisition of all these parameters is necessary for determining the risk associated to fibres exposition. A multidisciplinary routinely approach, based on the use of complementary simply-to-use but reliable analytical methods is the only possible strategy. In addition, the instrumental apparatus must be easily transportable on the field, directly on the mining site. The employment of specialized tools such as Polarized Light Microscopy associated to Dispersion Staining method (PLM/DS) and portable Raman spectroscopy for identification of environmental asbestos, are proved extremely effective in the improvement of the performance and rapidity of data acquisition and interpretation. Both PLM/DS and handheld Raman devices confirmed to be discriminant in the detection and characterization of asbestos fibres for both serpentine and amphibole. Furthermore, these techniques proved extremely effective even in the presence of strongly fibrous and altered samples.

Key-words (up to 6): asbestos; fibrous antigorite; *in situ* monitoring; dispersion staining; portable Raman; New Caledonia.

1. Introduction

Asbestos is the generic commercial definition for a group of naturally occurring mineral silicate fibres of the serpentine and amphibole groups. It includes the serpentine chrysotile (also known as “white asbestos”), and the amphibole minerals amosite (fibrous-asbestiform variety of grunerite, also known as “brown asbestos”), crocidolite (fibrous-asbestiform variety of riebeckite, commercially known as “blue asbestos”), as well as anthophyllite, tremolite and actinolite asbestos (IARC, 2012; EU, 2003). As a result of geological processes, Naturally Occurring Asbestos (NOA) is present in the natural environment, in rocks and soils, referring to mineral fibres that have not been extracted and refined for commercial purposes, but rather to asbestos that has been exposed unintentionally by excavation, road grading, or mining (Wagner, 2015; Bloise et al., 2016; Noonan, 2017). Weathering and human activity may disturb NOA-bearing rocks and release mineral fibres

into the air, which constitutes a potential risk to human exposure by inhalation (Cattaneo et al., 2012; Bayram et al., 2013; Cavallo and Rimoldi, 2013; Gualtieri et al., 2014; Vignaroli et al., 2014; Bloise et al., 2017; Gaggero et al., 2017; Noonan, 2017; Dichicco et al., 2018). The investigation of NOA started after the diagnosis of asbestos related pathologies in human populations non-occupationally exposed to asbestos (Browne and Wagner, 2001; Luce et al., 2004; Gunter et al., 2007; Harper, 2008; Culley et al., 2010; Thompson et al., 2011; Bayram et al., 2013). NOAs are known to be responsible for passive exposure of populations, which makes risk assessment and prevention plans more complex compared to professional exposure to asbestos. Actually, in environmental context, exposure is due to a large diversity of mineral fibres whose impact on the health of exposed people can be greater than the six-regulated asbestos minerals (Baris et al., 1978; Coffin et al., 1992; Comba et al., 2003; Gazzano et al., 2005; Groppo et al., 2005; Turci et al., 2005; Carbone et al., 2011; IARC, 2012, 2017). This results in a huge variability in chemical compositions and physical properties of the released fibres and therefore in a different reactivity in the organism for each case (Fubini and Otero Arean, 1999; Fubini and Fenoglio, 2007). The rising awareness on NOA related risk leads to a renewed interest in the *in situ* identification of regulated and non-regulated mineral fibres. The most common methods, listed in regulations and used by commercial-asbestos laboratories, have therefore to be applied to natural samples. Analysis of mineral fibres is a complex task which involves different approaches depending on the characteristic of the sample (*e.g.*, bulk, filter, soil, rock) and on the purpose of assessment (Nichols et al., 2002; Lee et al., 2008; Cavariani et al., 2010). Because of NOA heterogeneous composition, consisting of intermixed fibres morphologies and mineral phases, analytical investigation of mineral fibres requires a multidisciplinary analytical approach.

New Caledonia is one of the largest world producers of lateritic Ni-ores resulting from millions years alteration of ultrabasic rocks (Wacaster, 2011). According to current knowledge, the Boghen terrane in the central unit, the ultrabasic complex, and the northern metamorphic complex of the Grande Terre Island, are the main geological units most affected by the presence of asbestiform mineral fibres (Lahondère, 2007, 2012; DIMENC-SGNC, 2010). The occurrence of NOA-bearing rocks in more than one third of its surface area has been reported for over 20 years (INSERM U88, 1997). While (fibrous-asbestiform) tremolite is mainly present in central and northern Caledonia terranes, serpentine chrysotile and fibrous-lamellar antigorite occur in the peridotite complex (Fig. 1; Lahondère, 2007, 2012). Besides the environmental exposure to asbestos related to Ni mining's activity, a domestic exposure also exists. Remarkable is the case of the use of Pö in the past, a traditional white-coloured wall covering purely composed of asbestiform tremolite (Goldberg et al., 1991, 1995; Luce et al., 1994, 2000, 2004; Baumann et al., 2007, 2011; Houchot 2008).

Furthermore, recent statistical and epidemiological data display the presence of fibrous serpentines in tracks and soils as one of the most significant factors connected to risk (Baumann et al., 2011). The huge variety of asbestiform minerals and their distribution over a large part of the island make environmental asbestos a major public health issue for New Caledonia. A great work of survey of the different (fibrous) varieties of amphiboles and serpentines on the outcrops, resulting in a detailed geological map of natural occurrences, is ongoing (Lahondère, 2007, 2012; ANSES, 2010; DIMENC-SGNC, 2010).

To restrict the risk due to fibres exposition, the New Caledonia legislation (*Délibération n° 82 du 25 Août 2010*) included serpentine-antigorite in the list of the regulated-asbestos. Actually just preliminary data on its potential toxicity are available (ANSES, 2014; Tomatis et al., 2018). However, from a morphological point of view, recent studies confirm the fibrous-lamellar nature of Caledonian antigorite (CNRT - Laporte-Magoni et al., 2018)

In the assessment of the exposure risk, Caledonian mining companies developed a provisional monitoring prevention plan based on field geological survey, followed by an analytical laboratory investigation. The analytical procedure refers to methods provided by French regulation - NF X43-269 - for the air quality investigation in workplaces containing asbestos: Transmission (TEM) and Scanning Electron Microscopy (SEM) coupled with Energy Dispersive X-Ray Spectroscopy (EDS), and Phase Contrast Microscopy (PCM). However, no accredited laboratory is currently present in New Caledonia. Mineralogical-chemical characterization, counting and morphological investigations must be carried out abroad. Timing of analysis is therefore too long when compared to professional timelines. In this context, the on-field geological monitoring of asbestos and related minerals must be carried out in the most effective way. Thus, a dedicated classification based on descriptive criteria like colour, morphology, cohesion of rock, and fibre release was introduced by professional geologist to describe these asbestos-type occurrences. All these morphological-textural parameters depict an increasing *alteration status*, from non-altered (minimum degree of alteration) to highly altered (maximum degree of alteration), correlated with a potential rising risk resulting in a greater capability in the dispersion of fibres. Because of the wide range in natural shapes and morphologies presented by mineral fibres subjected to weathering, it seems very difficult to distinct with certainty the type of fibre. This operation requires a great deal of experience and an excellent mineralogical background. Subjectivity in the discrimination of morphological criteria and potential misinterpretation are therefore the main sources of error in the preliminary step of on-field identification. For example, misinterpretation in identification of asbestiform minerals might results in a commercial use of minerals analogous to the six-regulated asbestos (*e.g.*, quarry of white

asbestos near Rowland Flat, South Australia; Keeling et al., 2008, 2010; Fitz Gerald et al., 2010). Furthermore, the closely intergrowth of different asbestiform (and not) mineral phases complicates the field identification (Dogan and Emri, 2000; Groppo and Compagnoni, 2007a, 2007b; Rooney et al., 2018). Nowadays, there is a lack of a quantitative (or semi-quantitative) approach to classify the degree of alteration of the mineral fibres subjected to weathering. To improve the effectiveness and rapidity in the description of asbestos occurrences, and consequently to protect workers, an analytical *in situ* strategy appears necessary. Until now, rare isolated studies have been performed on the identification of asbestos using portable devices, usually involving portable Raman equipment (Jehlička et al., 2009; Bloise and Miriello, 2018). To our knowledge, there is no evidence of testing portable Raman spectroscopy for identification of asbestos-type minerals in lateritic units, associated to mining activity. The analytical challenge is to distinguish fibrous amphibole and serpentine minerals, including fibrous-lamellar antigorite, despite the high alteration levels of asbestos and laterite deposits.

This work aims to develop a diagnostic strategy, routinely applicable and able to discriminate and characterize the different species of asbestos. Attention was dedicated to Raman spectroscopy and Polarized Light Microscopy associated to Dispersion Staining method (PLM/DS), which offered the possibility to employ a portable or a benchtop equipment. Analytical performance of a handheld Raman device, to be used on field observation, was assessed against the more traditional mineralogical and petrological methods - such as optical microscopy, SEM, and TEM. Because of the importance of morphology and size distribution in the evaluation of the asbestiform nature, microscopic methods are crucial in the investigation of mineral fibres. PLM/DS is an optical routinely technique currently in use in investigation of Asbestos Containing Materials (ACMs) for the analysis of fibres concentrations of bulk building materials (EU 2003; Health and Safety Executive, 2006). On the other hand, it is not largely used with NOA samples (Baietto and Marini, 2018), especially for non-regulated mineral fibres (*e.g.*, antigorite, erionite, fluoro-edenite, balangeroite). Also in the case of amphiboles minerals, which are generally considered more simple to identify by PLM/DS, cummingtonite and winchite amphiboles may be confused with tremolite (Health and Safety Executive, 2006). In this respect, a specific work has been carried out to find the Refractive Index (RI) liquid which corresponds as much as possible to the RI value of antigorite. Finally, the impact of supergene alteration on the recognition of asbestiform minerals was evaluated, testing analytical methods even in presence of strongly fibrous and altered samples.

2. General Setting

2.1 The New Caledonia ultrabasic complex

The New Caledonia ophiolite complex is one of the largest in the world with best-exposed units of peridotite. The ultramafic peridotite complex, 300 km long, 50 km wide and 2 km thick, is certainly the most prominent terrane of New Caledonia (Ulrich et al., 2010). It is composed of a main massif – "Grand Massif du Sud" – located in the southernmost part of the island, and several tectonic klippes isolated by the erosion along the west coast (*e.g.*, Koniambo Massif; Fig. 1). This unit is dominantly formed of partially to totally hydrated upper mantle rocks, harzburgite-dunite and rare spinel- and plagioclase- lherzolite, with minor ultramafic (pyroxenite, wehrlite) and mafic cumulates (layered gabbros; Prinzhofer, 1981). The allochthonous unit is largely fractured and crosscut by dolerites, micro-diorites and various felsic dykes at all levels. Locally, amphibole lenses, about 200 m length and 10-50 m wide, appear at the base of serpentinite, above Poya basalt (Cluzel et al., 2012). As a consequence of cooling and low temperature hydration of the oceanic mantle lithosphere, the degree of serpentinization may range from 20 to 60 volume %. In addition, a more extensive serpentinization occurs also at the basal layer of the peridotite nappe, generally referred to as the tectonic *serpentinite sole*, consisting of a porphyroclastic mylonite (20-200 m thick) which likely formed during obduction (Avias, 1967; Orloff and Gonord, 1968; Rawling and Lister, 1999; Cluzel et al., 2012; Lagabrielle et al., 2013; Quesnel et al., 2016).

Despite the large number of geological studies existing on ophiolite of New Caledonia, a comprehensive understanding of mechanisms responsible for serpentinization is still lacking (Orloff and Gonord, 1968; Trescases, 1975; Barnes et al., 1978; Evans et al., 2013; Frost et al., 2013; Mothersole et al., 2017). Probably due to different thermodynamic conditions according to geodynamic context, several generations of serpentine minerals combined with minor amount of tremolite-amphibole may occur in the ultrabasic units, from the *serpentinite sole*, at the bottom, until the linked serpentines fractures, towards the top (Lahondère, 2007; Audet, 2008). Generally, serpentinized peridotites are cut by large fault planes with prismatic-lamellar crystals from centimetres to decimetres. These planes appear fresh and lamellae are parallel and welded together. Conversely, at the top of lateritic profile, close to pedolitic horizons, these blades become more altered, fragmented and associated with fibres that seem to be originated from the extreme cleavage (fraying) of these same lath-shaped crystals (Lahondère, 2007, 2012; Ulrich et al., 2010; Quesnel, 2015; Quesnel et al., 2016).

2.2 Laterite ore deposits

The ultramafic rocks of New Caledonia underwent weathering since early Miocene. Ni-laterite deposits were formed during the Miocene-Pliocene by lateritic weathering of obducted harzburgite-dunite peridotite nappe, in which both residual and absolute economic nickel concentration have resulted from supergene enrichment (Troly et al., 1979; Chevillotte et al., 2006). Ni-laterites formation starts with the emplacement and serpentinization of the ultramafic protolith, followed by exposure to a humid sub-tropical climate and the development of a deep intensely weathered regolith. From base to top, the weathering profile is composed of a saprock or saprolite horizon, a limonitic horizon, and a ferricrete at the top. Supergene Ni-ore deposits correspond to the hydrous Mg-Ni silicate-type ore and oxide-type ore depending upon the main Ni-bearing mineral phase, respectively exploited within the saprock/saprolite and at the base of the limonite horizon (Brand et al., 1998; Freyssinet et al., 2005; Butt and Cluzel, 2013; Trotet et al., 2015).

2.3 Asbestos occurrences in the ultrabasic units

According to Ulrich (2010), the basal *serpentinite sole* is dominated by lizardite (up to 90%), secondary chrysotile-polygonal serpentine, which occurrence consists of millimeter crack-seals veins, and antigorite, which only crystallized in veins. If the formation of the lizardite is assumed to be related to abyssal history of the ophiolite for the lherzolite, and to its supra-subduction history for the harzburgite, the origin of the antigorite veins is more questionable. Ulrich (2010) relates this contrasted serpentinization to an upward hydration of the peridotite nappe by metasomatic fluids released from the downgoing slab during the Eocene convergence. The occurrence of antigorite within the sole is interpreted as related to hotter fluid circulation (T >400 °C) when the HP-LT Diahot units were rising up beneath the ophiolite. This result accounts for the creation of a major rheological discontinuity forming the entire basal sole of the ultramafic sheet. Study on oxygen isotopes indicates that chrysotile was formed later, likely during obduction, by the circulation of meteoric fluids through micro-fractures (Ulrich, 2010), with higher water/rock ratios (Evans et al., 2013; Frost et al., 2013; Mothersole et al., 2017).

In laterite deposits, all main varieties of the serpentine group, associated to minor tremolite, have been observed. Owing to their ability to withstand better the oxidation processes, serpentine minerals are commonly found in saprolitic zone currently mined (Lahondère, 2012; Trotet, 2012). In the upper part of ultrabasic units, serpentinites generally outcrop along tectonic structural discontinuities as fractures, faults and shear zones (Leguere, 1976; Lahondère, 2012), even with

asbestiform habits (*e.g.*, fibrous antigorite; Lahondère, 2007). Antigorite is usually closely related to the main faulting pattern (Quesnel et al., 2016).

Caledonian minerals display a wide range of natural shapes, morphologies and *alteration status* depending on supergene alteration. Increasing the degree of alteration, a progressive loss of cohesion of massive assemblages leads to the disappearance of the original structure, until the appearance of individual asbestiform fibres. A mineralogical transformation process (formation of talc, silicification, etc.) can eventually occur (Lahondère, 2007). Furthermore, Figure 2 shows as assemblages displaying different degrees of alteration may exist simultaneously at the same outcrop.

3. Methodologies

3.1 New Caledonian samples

About 50 rock fragments collected in the mining site (outcrops, quarries, tracks, pit) of different ultrabasic units of Grande Terre Island (New Caledonia) were analyzed (Fig. 1; Table A). Samples, selected at different degree of alteration - from non-altered to maximum degree of alteration – consist in serpentines such as chrysotile and fibrous-lamellar antigorite, as well as (asbestos) tremolite-amphibole. Samples were collected at both *serpentinite sole* horizon (chrysotile) and in the lateritic profile (mainly antigorite and tremolite-actinolite). The on-field geological survey was realized by professional geologist of mining companies of New Caledonia using the mining nomenclature (CNRT - Laporte-Magoni et al., 2018, for details). Only the results of the eight most representative samples, coming from Tontouta (west coast) and Poro (east coast) mines, are displayed in this work, as reported in Table 1.

3.2 Analytical monitoring strategy

3.2.1 Microscopies

Secondary electron imaging (SEI) and semi-quantitative Energy dispersive X-ray spectroscopy (EDS) microanalysis were carried out on both natural samples and petrographic thin sections with different Scanning Electron Microscopes (SEM): i) JEOL JSM-IT 300 LV/LA with Low Vacuum Mode equipped with an Oxford-X-Max EDS, available at ISEA Laboratory, University of New Caledonia; ii) LEICA 430i equipped with an ISIS EDS microanalysis and ZEISS EVO 40 equipped with Oxford-INCA EDS, available at the accredited Laboratory of Arpae – Agenzia regionale per la prevenzione, l'ambiente e l'energia dell'Emilia Romagna, Reggio Emilia, Italy; and iii) JEOL 6400 equipped with an Oxford-INCA EDS, at Department of Chemistry, Life Sciences and

Environmental Sustainability, University of Parma. SEI images were acquired at various magnifications and accelerating voltages, commonly 5-25 kV depending on the instrument used. Before the analysis samples were coated with 10 nm carbon layer.

Micrographs and TEM were performed with two instruments. i) JEOL ARM 200F Scanning Transmission Electron Microscope (STEM), at Department of Materials Chemistry, National Institute of Chemistry, Ljubljana, Slovenia, using a probe Cs corrected STEM, model ARM 200F mounting a high-brightness Cold Field Emission Gun (CFEG) operating at 80 kV. The microscope was equipped with an EDS system (Centurio 100 mm2, JEOL). Analyses were conducted in TEM mode together with Selected-Area Electron Diffraction (SAED) and EDS analysis to identify chrysotile fibres (>20 fibres for each sample performed). In addition to common TEM identification (Imaging, SAED and EDS) of asbestos fibres, Bright Field (BF) and Medium Angle Annular Dark Field (MAADF) STEM coupled with EDS mapping have been applied. All the samples were tested for stability under the electron beam and the observations were made accordingly. ii) JEOL JEM 2010 equipped with an Oxford-INCA 100 EDS, available at the CIGS Laboratory, University of Modena and Reggio Emilia. The microscope operating at 100 kV, was equipped with a double tilt holder. The samples were transferred on a lacey carbon mesh copper grid (300 mesh). A small quantity of samples was suspended in 2-propanol and ground for two minutes. The suspension was transferred in an Eppendorf's tube followed by a mild sonication for two minutes to obtain a homogeneous suspension. Two drops of the suspension were transferred on the TEM grid.

PLM analyses, coupled with Dispersion Staining method of observation (PLM/DS) and equipped with a phase contrast mask, were performed at the accredited laboratory of Arpae, at Reggio Emilia, in Italy. Two microscope equipment Leica DIALUX 20 EB and Leica DM4 B have been used for the qualitative observations of samples. Each fibre type, sampled by selecting a few representative fibres or bundles, was placed on a microscope-slide. Identification occurs with the oil immersion method, using the following Refractive Indices: RI 1.550 for chrysotile, RI 1.580 (recommended by Italian regulation - D.M. 06/09/94) and 1.605 (advised by UK - Health and Safety Executive, 2006) for tremolite, and the intermediate RI 1.5680 for non-chrysotile serpentine.

3.2.2 Raman spectroscopy

Non-polarized micro-Raman spectra have been obtained on petrographic thin sections in nearly backscattering geometry with a Horiba Jobin-Yvon LabRam apparatus, equipped with an Olympus microscope with 10x, 50x, Ultra-Long Working Distance 50x, and 100x objectives and a motorized x-y stage. The 632.8-nm line of a He–Ne laser and the 473.1-nm line of a doubled Nd:YAG diode

pumped laser have been used as excitation; laser power has been controlled by means of a series of density filters, in order to avoid heating effects. The minimum lateral resolution was about 1 μm (with the 100x objective); the depth resolution was set to few microns by means of a confocal hole. The spectral resolution is about 2 and 4 cm^{-1} at the 632.8 and 473.1 nm excitation wavelengths, respectively. The system was calibrated using the 520.7 cm^{-1} Raman peak of silicon before each experimental session. In addition, in the high wavenumber range, the spectra were constantly calibrated using spectral lamps. The 632.8-nm line was mostly used to obtain high-resolution spectra in the low wavenumber range (100-1200 cm^{-1}), whereas the 473.1-nm source was utilized to enhance the OH stretching signal of the water molecules in the high wavenumber range (3000-4000 cm^{-1}). The spectra were collected using the 100x objective with repeated acquisition: 5 acquisitions for 30 s and 15 for 10 s in the low and high wavenumber spectral range, respectively.

Raman *in situ* measurements were carried out with an handheld Enspectr RaPort® Raman instrument, weighing 2.1 kg, equipped with a 532-nm laser at maximum output power of 30 mW. Raman spectra have been obtained over the wavenumber range 100-4000 cm^{-1} with a spectral resolution of 8 cm^{-1}. The instrument is remotely controlled via a USB 2.0 cable connected to a laptop. The spectra were collected in a single acquisition up to 60 s. The instrument self-calibrate automatically before each set of measurements. Taking into account the large laser spot (about 1 mm) and the lack of rigid mounts for positioning, a real spatial resolution in the range of few cubic millimeter is expected. This could be a disadvantage when analysing very small features or heterogeneous materials. On the other hand, as we had a large volume of scattering, it was easy to focus the laser beam on the bundles of fibres. Working off-line, the long battery life permits an autonomous operation up to 6 hours. A temperature range of 0-40 °C is recommended during operation on field.

The background subtraction on each spectrum was performed with LabSpec® software.

4. Results

4.1 Macroscopic description of samples

At the hand scale, samples of New Caledonia show an evident lack of cohesion and an altered appearance. Compared to most of the worldwide NOA-occurrences (*e.g.*, Western Alps, Haute-Corse; ANSES, 2010), they are generally more friable and characterized by a structureless aspect (Fig. 3 d,e,h). Chrysotile (Sample 57) is in the form of little veins and veinlets (up to 5 mm wide) cross-cutting serpentinized peridotite (Fig. 3a). It commonly shows a reddish-colour, alternating sub-millimeter sized pale-brown–black–reddish banding. This is the typical appearance of

chrysotile that professional geologists expect on the outcrops for its identification. Samples classified as non-altered antigorite (minimum degree of alteration – Sample 13; Fig. 3c) display a compact, moderately hardened appearance, dominated by a pale-green to green colour. Platy shaped lamellae are welded and parallel to each other. Increasing the alteration, antigorite shows a more friable aspect, coupled with the presence of bundles of laminas. Samples show a massive to structureless appearance, from white to pale-green colour (Sample 6; Fig. 3d). The most altered samples, instead, appear fibrous and characterized by porous low density material; fibrous-lamellar blades occur randomly orientated to form aggregates and bundles (Sample 35; Fig. 3e). On the other hand, tremolite fragments show only a little variation in morphology as the degree of alteration increases. Tremolite samples are characterized by compacted, massive to moderately hardened appearance, from green to pale-green–whitish colour. They exhibit a columnar morphology, characterized by the overlapping of well-formed prismatic crystals. Several individual fibres have also been observed (Sample 41; Fig. 3g). Furthermore, increasing the alteration status, tremolite appear more fractured (Sample 36; Fig. 3h).

4.2 Evaluation of the performance of portable Raman in the identification of altered minerals.

A set of preliminary measurements devoted to testing the performance of the handheld Raman equipment was carried out in laboratory on all the rock-fragments. One or at least two spot analyses were performed for each sample. On 47 analysed samples, 41 were successfully identified, allowing the discrimination of the main serpentine or amphibole phase. As illustrated in Figure 4, spectra obtained for tremolite samples show the worst signal-to-noise ratio, compared to those of serpentines (Fig. 5), due to increased fluorescence interference. By the way, the identification of the predominant phase was not compromised (Table 2). Concerning measurements realized on the most altered serpentine and amphibole, on 15 very altered samples (maximum degree of alteration), only 4 were not identified with portable Raman equipment. Despite the complete loss of cohesion of altered samples, the quality of data was not affected, allowing the identification of the mineral phase (Fig. 4).

To verify the user-friendliness of the Raman portable device, it was successfully tested at the open pit of Tontouta, in New Caledonia. On 30 spot analyses, 20 were positively identified. Samples of antigorite, chrysotile and altered serpentine, probably saponite, have been identified. Figure 5 shows an example of a raw Raman spectrum obtained in real-time measurement (Raport instrument, 532-nm laser) compared with a spectrum recorded with the laboratory Raman microspectrometer (473.1-nm laser). The micro-Raman spectrum was acquired on a bundle of fibrous-lamellae choosing the optimal conditions of measurement (*e.g.*, spot analysis, objective 100x, time and

number of acquisitions, filter, etc.). On the contrary, the portable Raman does not allow the choice of all these instrumental parameters. In this latter case, the acquisition was performed directly on fibre bundles, selecting only the time of acquisition. Despite all intrinsic instrumental differences, spectra appear perfectly comparable at both low- and high-wavenumber regions, allowing the identification of the mineral phase (Rinaudo et al., 2003; Auzende et al., 2004; Groppo et al., 2006; Petriglieri et al., 2015). The presence in the OH-stretching region of the typical doublet, with the main peaks located at about 3665 and 3695 cm^{-1} of antigorite, confirm with certitude the discrimination of this serpentine phase (Petriglieri et al., 2015; Tarling et al., 2018). Only a slightly fluorescence interference occurs.

4.3 Identification of fibrous minerals by PLM/DS.

The impossibility of estimating the potential of fibre emission from a field survey suggests to develop a technique able to identify and evaluate the release of potentially asbestiform fibres into the environment. In this respect, PLM/DS represents the most suitable microscopic technique transposable on field sites. However, there are no published data on antigorite analysis by PLM/DS. No guidelines are provided by regulations for the discrimination of fibrous antigorite. About Caledonian asbestos, chrysotile fibres (Sample 57) have been investigated with the typical RI 1.550 liquid (Fig. 6). Observed in phase contrast mode, fibres exhibit the characteristic pale-blue colour with an orange halo (Fig. 6a), whereas they appear blue to purple in dark field observation (Fig. 6b). Asbestos tremolite have been analysed with RI 1.580 and RI 1.605 liquids. Tremolite must be better identified with RI 1.605, according to UK - Health and Safety Executive (2006). Observed in phase contrast mode, fibres exhibit a pale-blue to dark-grey colour, often coupled with an orange halo. Moreover, they appear yellow to purple in dark field observation mode (Fig. 7). On the other hand, a specific work aimed to find the RI liquid that match most closely the refractive index value of antigorite has been carried out. Lizardite has a mean RI between 1.54 and 1.55, while the lath-shaped lamellae of antigorite generally show a higher RI, on average 1.566 (Deer et al., 1992). We tested RI 1.5680 for the discrimination of antigorite: in phase contrast observation fibres show a pale-blue to white colour, without halo (Fig. 6c), whereas under dark field they have a blue indigo colour (Fig. 6d). The RI 1.5680 proved to be the RI liquid that mostly matches the antigorite phase, showing characteristic dispersive colours which allow to distinguish antigorite from chrysotile. Applying this methodology to more fibres for each sample, we could therefore assume that also minor fibrous phases will be detected.

4.4 Complex mineralogy and morphology of Caledonian mineral fibres

Comparing data obtained by laboratory investigation with the on-field survey based on morphological-textural criteria, most of samples reveal a different and more complex mineralogical nature, as reported in Table 2, and Table A.

In the identification of asbestiform serpentine phases, Sample 33 had a crucial role in the discrimination of chrysotile from fibrous antigorite. Macroscopically identified as non-altered antigorite (minimum degree of alteration), this sample appears pale-green to white at the hand-sample scale, formed by the overlay of parallel and welded well-grown lamellae (Fig. 3b). Contrary to expectation, all analytical techniques confirm that it is chrysotile (Table 2). Petrographic observations show the typical zebra-like appearance of chrysotile samples, according to Wicks and Whittaker (1977). At stereo-microscope, well-formed blades occur. Actually, only after a softly mechanical stress, using tweezers, a woolly-like appearance has been recorded (Fig. 8a). PLM/DS observations on mount particles confirm the identification of chrysotile fibre using the standard RI 1.550 liquid. Fibres observed in phase contrast mode exhibit the typical pale-blue colour with the orange halo (Fig. 8b), and appear blue to purple in dark field observation. Increasing the magnification, SEI images display a compact bundle of parallel fibrils of chrysotile. Fibrils are tightly welded and an unusual high density of tubes has been recorded (Fig. 8d). A careful observation of fracturing and cleavage highlights the presence of thin fibrils. As illustrated in the Figure 9 the identification of chrysotile was confirmed by TEM-SAED analysis. TEM is the only instrument capable of imaging the hollow-core of chrysotile fibrils. Furthermore, both micro-Raman spectroscopy and portable Raman equipment were applied on this sample, allowing the identification of the chrysotile variety (Fig. 8c).

Moreover, most of rock-fragments macroscopically identified as monomineralic are actually composed of a strictly association of serpentine and amphibole phases. Even tremolite specimens show systematically the closely intergrowth with secondary antigorite and/or chrysotile serpentine (Table A). Concerning samples identified as antigorite, on 32 specimens, 17 display a more complex nature consisting of a closer association of fibrous-lamellar antigorite and chrysotile-serpentine. Among these, two samples are made up of chrysotile only (Table A).

We report, as example, the case of Sample 30 (Fig. 10). Identified by professional geologist as massive antigorite (non-altered; Fig. 3f), the petrographic observation with SEM images reveals its complex nature consisting of a strictly intergrowth of fibrous-lamellar of antigorite and randomly oriented flexible fibres of chrysotile-type. Moreover, micro-Raman analysis confirms this result,

showing the typical Raman spectra of both chrysotile and antigorite serpentine minerals (Fig. 10; (Auzende et al., 2004; Petriglieri et al., 2015). In OH-stretching region (3550-3850 cm^{-1}) chrysotile displays the main peak at 3698 cm^{-1} with a shoulder at about 3691 cm^{-1}. Antigorite shows the diagnostic doublet with the main peaks located at about 3665 and 3695 cm^{-1}, allowing the discrimination of the two phases.

4.5 Underestimation of fibrous nature of Caledonian samples.

SEM images, acquired especially in SEI mode on lower voltage (5 kV), allow to investigate more in details the surface features of Caledonian samples. Even non-altered antigorite samples (*e.g.*, Sample 13, 33; Fig. 3b,c) show the presence of flexible thin, potentially breathable, fibres at the surface (Fig. 11). From the point of view of regulation and health, these fibres should be counted as breathable elongated particles, according to WHO dimensional criteria (Length >5 μm, Diameter <3 μm, L/D ≥ 3:1, under optical microscopy; IARC, 2012). Performing PLM/DS on apparently lamellar, non-altered samples, would allow to confirm (or exclude) preliminarily the fibrous, potentially asbestiform, habit of asbestos and related minerals, as demonstrated by Caledonian samples (Figs. 6 and 8). It should be noted that conforming to the classification adopted by mining companies, no samples display the visual features generally attributed to a lack of alteration. All samples identified as non-altered, and therefore not hazardous, actually display potentially breathable fibres at the surface. Furthermore, increasing the alteration status, a greater capacity in the release of fibres was recorded.

5. Discussion

In the context of mining professional sector, the development of a user-friendly reliable strategy, able to discriminate the potential asbestiform fibres from non-harmful fragments, is the first requisite in the implementation of the actual monitoring prevention plan. Data achieved describe a complex situation. Comparing laboratory results with the on-field geological survey, based on morphological-textural criteria, most of samples reveal a different and more complex mineralogical nature. Therefore, the monitoring prevention plan currently in use is not sufficient for discriminating asbestos from non-asbestos elongated particles. Each instrument implies advantages and limits. This means that a multidisciplinary approach is the only possible strategy to answer to worker and population requirements. At present, there is not a technique capable to fully characterize an asbestos fibre on the outcrop, providing information about size, morphology, chemical composition and alteration grade. On the other hand, the acquisition of chemical-structural and morphological information is necessary for determining the risk associated to fibre exposition.

The employment of specialized tools such as portable Raman spectrometer and PLM/DS microscopy proved extremely effective, even on field testing directly at the mining front, for both serpentine and amphibole. The identification of the more or less altered varieties occurs immediately, with rapid acquisitions (from few seconds to minutes) directly on the fibres (or on lamellae) embedded in their textural context. Moreover, a little training is required to operators for the employment of these methods. The implementation of two complementary analytical methodologies could be the answer for the discrimination of complex samples. In this respect, the analytical performances of portable Raman and PLM/DS were compared with laboratory strategies, generally involved by accredited asbestos laboratories.

According to published literature, Raman spectroscopy has proved to be very sensitive to variations in chemical composition, allowing the discrimination of asbestos (Bard et al., 2004; Rinaudo et al., 2005; Petry et al., 2006) and related mineral fibres (Groppo et al., 2006) in NOA context. Moreover, due to its high resolution power, it can be successfully used not only on massive specimens, but also in the investigation of fibre bundles and/or single micrometre-sized fibres (fibre of 1-2 μm in diameter; Bard et al., 1997; Rinaudo et al., 2005; Musa et al., 2012; Croce et al., 2013). To obtain high-quality spectra the laser beam must be accurately focused on the area of interest. Especially in the cases of most fibrous and altered fragments, the laser beam should be focused on non-cohesive aggregates of randomly orientated fibrous-lamellae. Compared to laboratory Raman micro-spectrometer, the handheld device does not allow the choice of different instrumental parameters, selecting only the time of acquisition. Despite remarkable differences in spatial (1 mm and 1-2 μm, respectively) and spectral resolution (8 cm^{-1} and 4 cm^{-1}, respectively), spectra appear comparable at low- and high-wavenumber, allowing the identification of the mineral phase. The acquisition of spectra in the extended wavenumber range (100-4000cm^{-1}) allows to identify with certitude serpentine and amphibole. OH-stretching is a very sensitive probe for the micro-structure investigation of asbestos minerals. Fluorescence emission phenomena and the difficulty to point and/or focus laser beam on a non-cohesive bundles of fibres are the major disadvantages generally occurring during measurement.

If handheld Raman equipment requires more attention during measurement, PLM/DS need free asbestos fibres for sample preparation. PLM/DS observations on mount particles allowed to successfully identify all fibrous samples analysed, confirming as a diagnostic method also in investigation of natural samples. PLM/DS provides information about mineralogical identification and morphology of fibres and/or lamellae. Moreover, the implementation of RI 1.5680 in regulated protocols would also allow to discriminate (fibrous) antigorite from chrysotile (RI 1.550). PLM/DS

analysis is relatively low cost and widely available. It offers great sensitivity even at very low concentrations and generally differentiates the non-asbestiform and asbestiform habits. With careful application of this method, a single fibre may be found in a few milligrams of dispersed material. In theory, for a fibre about 100 μm long and about 2 μm diameter, a detection limit in the order of 1 ppm by mass is expected (Health and Safety Executive, 2006). Repeating in routine this simple and rapid technique on more particles for each sample, PLM/DS may be an efficient tool in the characterization of asbestos in rocks. By contrast, its main limit is essentially related to detection of smaller particles. While PLM/DS allows to investigate different population of particles in the range of micrometer scale (10-300 μm), electron microscopies give information down to nanometric scale (TEM resolution, 0.01-10 μm; Cavariani et al., 2010).

Even if electron microscopies are known for their high diagnostic power in the full characterization of small particles at different magnifications, they are no suitable to be routinely applied at the field level, requiring skilled microscope operators, several time for sample preparation and data acquisition, and high analytical costs. Moreover, they allow to analyse very little specimens, too little compared to the outcrop volume (Cavariani et al., 2010).

Generally involved in evaluation of asbestos concentrations, SEM enables the quantity (size and distribution), morphology, and semi-quantitative composition (EDS system) of asbestos fibres (Cossio et al., 2018). Compared to optical microscopy, SEM has an increased depth in field, which allows extending the particle resolution down to approximately 0.1 μm - at one order of magnitude smaller than optical microscopy. Sub-millimetric sized fibres and cleavage fragments should be so investigated. SEM images, acquired especially in SEI mode on lower voltage (5-10 kV) have proved effective in the description of intermediate and fibro-lamellar morphologies, especially for fibrous antigorite investigation. Concerning semi-quantitative chemical analyses, EDS allows to distinguish easily amphibole from serpentine. Moreover, chemical differences between serpentine phases were confirmed to be generally insignificant compared to natural variability within individual serpentine phases, according to published literature (Schreier, 1989; Cavallo and Rimoldi, 2013; Wagner, 2015). The most complete method in the characterization of asbestos is TEM, which combine morphological information (TEM imaging) to chemical data (EDS) and crystallographic characterization (SAED). Only at TEM-scale it is possible to investigate certain structural details. Nevertheless, from a statistical point of view the acquisition of a few SAED patterns is not representative in the evaluation of polytypes percentage. It allows however to analyse very small volumes, so the homogenisation of the sample is crucial if the results are representative of the entire sample. Furthermore, detailed structural and chemical characterization of asbestos

minerals is very difficult to tackle for the small dimensions and similarity of crystals, the instability under several analytical probes and the extremely variable chemical composition, even within a single fibre itself. Electron microscopies are complex and expensive. Due to their own complexity, an extensive operator training is required. TEM's high performances make it perfectly suitable for research. Unfortunately, the impossibility to be used as a routine analysis let its employment hard in New Caledonia mining context.

5. Conclusion

The development of a diagnostic analytical strategy, routinely applicable in mining activity is the first requirement in the implementation of the current monitoring to prevention plan. To date there is not a technique capable to characterize an asbestos fibre *in situ*, providing information about size, morphology, chemical composition and alteration grade. However, the acquisition of all these parameters is necessary for determining the risk associated to fibres exposition. A multidisciplinary routinely approach, based on the use of complementary easy-to-use, but reliable methods is the only possible strategy. In addition, the instrumental apparatus must be easily transportable on-field, directly on the mining site. The employment of specialized tools such as Polarized Light Microscopy associated to Dispersion Staining method (PLM/DS) and portable Raman spectrometer for identification of environmental asbestos proved extremely effective in the improvement of the performance and rapidity of data acquisition and interpretation. Both PLM/DS and handheld Raman equipment confirmed to be discriminant in the detection and characterization of asbestos fibres for both serpentine and amphibole. Furthermore, these techniques proved extremely effective even in the presence of highly fibrous and altered samples. PLM/DS observations allowed to successfully identify all fibrous samples analysed, providing information about the mineralogical identification and the morphology of fibres and/or lamellae. Using the Refractive Index 1.5680 liquid it is also possible to discriminate (fibrous) antigorite from chrysotile (RI 1.550). Repeating analysis on more particles, PLM/DS may be an efficient tool in characterization of natural asbestos. Raman spectroscopy confirms to be a power diagnostic tool in the identification of the main varieties of the serpentine and amphibole families. Tests realized in mining context at the open pit of Tontouta (New Caledonia), have confirmed its high diagnostic power. To guarantee the optimal employment of both these devices, a training formation of the operators is required. An analytical routinely protocol based on the use of complementary methods allows to ensure the successfully identification of samples observed. All these considerations may applied to all type of unconfined sites of exposition, including environmental and domestic expositions.

Acknowledgments

This work was supported by the CNRT "Nickel and its environment" of New Caledonia. We are grateful to *Scansetti Centre* (Interdepartmental Center for Studies on Asbestos and other Toxic Particulates, University of Torino, Italy), *Arpae Emilia-Romagna* (Agenzia regionale per la prevenzione, l'ambiente e l'energia dell'Emilia Romagna, Reggio Emilia, Italy), and *University of Milano-Bicocca* (Italy) for research collaborations and thoughtful discussions. We also thank the *Comité Interminier Amiante* and the mining society *Société Minière Montagnat* of New Caledonia for its support and assistance in this project. Our sincere thanks to referees for constructive comments and suggestions, which greatly improved the manuscript.

References

ANSES, 2010. Affleurements naturels d'amiante. État des connaissances sur les expositions, les risques sanitaires et pratiques de gestion en France et à l'étranger. Maisons-Alfort, France, 248 pp.

ANSES, 2014. Évaluation de la toxicité de l'antigorite. Maisons-Alfort, France, 116 pp.

Audet, M.-A., 2008. Le massif du Koniambo, Nouvelle-Calédonie Formation et obduction d'un complexe ophiolitique du type SSZ. Enrichissement en nickel, cobalt et scandium dans les profils résiduels. PhD thesis, Université de la Nouvelle Calédonie and Université du Quebec a Montreal, 355 pp.

Auzende, A.L., Daniel, I., Reynard, B., Lemaire, C., Guyot, F., 2004. High-pressure behavior of serpentine minerals: A Raman spectroscopic study. Physics and Chemistry of Minerals, 31, 269-277.

Avias, J., 1967. Overthrust structure of the main ultrabasic New Caledonia massives. Tectonophysics, 4, 531-541.

Baietto, O., Marini, P., 2018. Naturally occurring asbestos: Validation of PCOM quantitative determination. Resources Policy, 1-6.

Bard, D., Yarwood, J., Tylee, B., 1997. Asbestos fibre identification by Raman microspectroscopy. Journal of Raman Spectroscopy, 28, 803-809.

Bard, D., Tylee, B., Williams, K., Yarwood, J., 2004. Use of a fibre-optic probe for the identification of asbestos fibres in bulk materials by Raman spectroscopy. Journal of Raman Spectroscopy, 35, 541-548.

Baris, Y.I., Sahin, A.A., Ozesmi, M., Kerse, I., Ozen, E., Kolacan, B., Altinörs, M., Göktepeli, A., 1978. An outbreak of pleural mesothelioma and chronic fibrosing pleurisy in the village of Karain/Urgup in Anatolia. Thorax, 33, 181-192.

Barnes, I., O'neil, J.R., Trescases, J.-J., 1978. Present day serpentinization in New Caledonia, Oman and Yugoslavia. Geochimica et Cosmochimica Acta, 42, 144-145.

Baumann, F., Rougier, Y., Ambrosi, J.P., Robineau, B.P., 2007. Pleural mesothelioma in New Caledonia: an acute environmental concern. Cancer Detection and Prevention, 31, 70-76.

Baumann, F., Maurizot, P., Mangeas, M., Ambrosi, J.-P., Douwes, J., Robineau, B.P., 2011. Pleural mesothelioma in New Caledonia: associations with environmental risk factors. Environmental health perspectives, 119, 695-700.

Bayram, M., Dongel, I., Bakan, N.D., Yalçin, H., Cevit, R., Dumortier, P., Nemery, B., 2013. High risk of Malignant Mesothelioma and pleural plaques in subjects born close to ophiolites. Chest, 143, 164-171.

Bloise, A., Miriello, D., 2018. Multi-analytical approach for identifying asbestos minerals in situ. Geosciences, 8, 1-11.

Bloise, A., Punturo, R., Catalano, M., Miriello, D., Cirrincione, R., 2016. Naturally occurring asbestos (NOA) in rock and soil and relation with human activities: The monitoring example of selected sites in Calabria (southern Italy). Italian Journal of Geosciences, 135, 268-279.

Bloise, A., Catalano, M., Critelli, T., Apollaro, C., Miriello, D., 2017. Naturally occurring asbestos: potential for human exposure, San Severino Lucano (Basilicata, Southern Italy). Environmental Earth Sciences, 76, 648-661.

Brand, W.N., Butt, C.R.M., Elias, M., 1998. Nickel laterites: Classification and features. Journal of Australian Geology & Geophysics, 17, 81-88.

Browne, K., Wagner, J.C., 2001. Environmental exposure to amphibole-asbestos and mesothelioma. Canadian Mineralogist, 5, 21-28.

Butt, C.R.M., Cluzel, D., 2013. Nickel laterite ore deposits: weathered serpentinites. Elements, 9, 123-128.

Carbone, M., Baris, Y.I., Bertino, P., Brass, B., Comertpay, S., Dogan, A.U., Gaudino, G., Jube, S., Kanodia, S., Partridge, C.R., Pass, H.I., Rivera, Z.S., Steele, I., Tuncer, M., Way, S., Yang, H., Miller, A., 2011. Erionite exposure in North Dakota and Turkish villages with mesothelioma. Proceedings of the National Academy of Sciences, 108, 13618-13623.

Cattaneo, A., Somigliana, A., Gemmi, M., Bernabeo, F., Savoca, D., Cavallo, D.M., Bertazzi, P.A., 2012. Airborne concentrations of chrysotile asbestos in serpentine quarries and stone processing facilities in Valmalenco, Italy. Annals of Occupational Hygiene, 56, 671-683.

Cavallo, A., Rimoldi, B., 2013. Chrysotile asbestos in serpentinite quarries: a case study in Valmalenco, Central Alps, Northern Italy. Environmental science. Processes & impacts, 15, 1341-50.

Cavariani, F., Marconi, A., Sala, O., 2010. Asbestos: sampling, analytical techniques and limit values. Italian Journal of Occupational and Environmental Hygiene, 1, 18-29.

Cluzel, D., Aitchison, J.C., Picard, C., 2001. Tectonic accretion and underplating mafic terranes in the late Eocene intraoceanic fore-arc of New Caledonia (Southwest Pacific): Geodynamic implications. Tectonophysics, 340, 23-59.

Cluzel, D., Maurizot, P., Collot, J.Y., Sevin, B., 2012. An outline of the Geology of New Caledonia; from Permian-Mesozoic Southeast Gondwanaland active margin to Cenozoic obduction and supergene evolution. Episodes, 35, 72-86.

Coffin, D.L., Cook, P.M., Creason, J.P., 1992. Relative mesothelioma induction in rats by mineral fibers: comparison with residual pulmonary mineral fiber number and epidemiology. Inhalation Toxicology, 4, 273-300.

Comba, P., Gianfagna, A., Paoletti, L., 2003. Pleural Mesothelioma cases in Biancavilla are related to a new fluoro-edenite fibrous amphibole. Archives of Environmental Health, 58, 229-232.

Cossio, R., Albonico, C., Zanella, A., Fraterrigo-Garofalo, S., Avataneo, C., Compagnoni, R., Turci, F., 2018. Innovative unattended SEM-EDS analysis for asbestos fiber quantification. Talanta, 190, 158-166.

Croce, A., Musa, M., Allegrina, M., Rinaudo, C., Baris, Y.I., Dogan, A.U., Powers, A., Rivera, Z., Bertino, P., Yang, H., (2013). Micro-Raman spectroscopy identifies crocidolite and erionite fibers in tissue sections. Journal of Raman Spectroscopy, 44, 1440-1445.

Culley, M.R., Zorland, J., Freire, K., 2010. Community responses to Naturally Occurring Asbestos: Implications for public health practice. Health Education Research, 25, 877-891.

Deer, W.A., Howie, R.A., Zussman, J., 1992. An introduction to the rock-forming minerals, 2. Ed. Hong Kong, Longman Scientific & Technical, 696, 712 pp.

Délibération n° 82 du 25 août 2010 - Relative à la protection des travailleurs contre les poussières issues de terrains amiantifères dans les activités extractives, de bâtiment et de travaux publics. JONC du 9 Septembre 2010.

Dichicco, M.C., Laurita, S., Sinisi, R., Battiloro, R., Rizzo, G., 2018. Environmental and health: the importance of tremolite occurence in the Pollino Geopark (Southern Italy). Geosciences, 8, 98-110.

DIMENC-SGNC, 2010. Cartographie des terrains potentiellement amiantifères en Nouvelle-Caléconie - Etat des connaissances, Mars 2010. DIMENC-SGNC, BRGM, Nouméa, Nouvelle Calédonie.

Dogan, M., Emri, S., 2000. Environmental health problems related to mineral dusts in Ankara and Eskisehir, Turkey, Yerbilimleri, 22, 149-161.

EU, 2003. Directive 2003/18/EC of the European Parliament and of the Council of 27 March 2003 amending Council Directive 83/477/EEC on the protection of workers from the risks related to exposure to asbestos at work. Official Journal L 097, 15/04/2003 P.0048-0052

Evans, K.A., Powell, R., Frost, B.R., 2013. Using equilibrium thermodynamics in the study of metasomatic alteration, illustrated by an application to serpentinites. Lithos, 168-169, 67-84.

Fitz Gerald, J.D., Eggleton, R.A., Keeling, J.L., 2010. Antigorite from Rowland Flat, South Australia: asbestiform character. European Journal of Mineralogy, 22, 525-533.

Freyssinet, P., Butt, C.R.M., Morris, R.C., Piantone, P., 2005. Ore-forming processes related to lateritic weathering. In: Hedenquist, J.W., Thomson, J.F.H., Goldfarb, R.J., Richards, J.P. (Eds.), Economic Geology 100th Anniversary Volume. Economic Geology Publishing Company, New Haven, Connecticut, pp. 681-722.

Frost, B.R., Evans, K.A., Swapp, S.M., Beard, J.S., Mothersole, F.E., 2013. The process of serpentinization in dunite from New Caledonia. Lithos, 178, 24-39.

Fubini, B., Fenoglio, I., 2007. Toxic Potential of Mineral Dusts. Elements, 3, 407-414.

Fubini, B., Otero Arean, C., 1999. Chemical aspects of the toxicity of inhaled mineral dusts. Chemical Society Reviews, 28, 373-381.

Gaggero, L., Sanguineti, E., Yus González, A., Militello, G.M., Scuderi, A., Parisi, G., 2017. Airborne asbestos fibres monitoring in tunnel excavation. Journal of Environmental Management, 196, 583-593.

Gazzano, E., Riganti, C., Tomatis, M., Turci, F., Bosia, A., Fubini, B., Ghigo, D., 2005. Potential toxicity of nonregulated asbestiform minerals: balangeroite from the Western Alps. Part 3: Depletion of antioxidant defenses. Journal of Toxicology and Environmental Health, Part A, 68, 41-49.

Goldberg, P., Goldberg, M., Marne, M.J., Hirsch, A., Tredaniel, J., 1991. Incidence of pleural mesothelioma in New Caledonia: a 10-year survey (1978–1987). Archives of Environmental Health, 46, 306-309.

Goldberg, P., Luce, D., Billon-Gailland, M.A., Quénel, P., Salomon-Nekiriai, C., Nicolau, J., 1995. Identification d’un excès de risque de cancer de la plèvre en Nouvelle-Calédonie lié à l’exposition environnementale et domestique à la trémolite. Revue d'epidémiologie et de santé publique, 43, 444-450.

Groppo, C., Compagnoni, R., 2007a. Metamorphic veins from the serpentinites of the Piemonte Zone, Western Alps, Italy: a review. Periodico di Mineralogia, 76, 127-153.

Groppo, C., Compagnoni, R., 2007b. Ubiquitous fibrous antigorite veins from the Lanzo Ultramafic Massif, Internal Western Alps (Italy): characterisation and genetic conditions. Periodico di Mineralogia, 76, 169-181.

Groppo, C., Tomatis, M., Turci, F., Gazzano, E., Ghigo, D., Compagnoni, R., Fubini, B., 2005. Potential toxicity of nonregulated asbestiform minerals: Balangeroite from the Western Alps. Part 1: Identification and characterization. Journal of Toxicology and Environmental Health - Part A, 68, 1-19.

Groppo, C., Rinaudo, C., Cairo, S., Gastaldi, D., Compagnoni, R., 2006. Micro-Raman spectroscopy for a quick and reliable identification of serpentine minerals from ultramafics. European Journal of Mineralogy, 18, 319-329.

Gualtieri, A.F., Pollastri, S., Gandolfi, N.B., Ronchetti, F., Albonico, C., Cavallo, A., Zanetti, G., Marini, P., Sala, O., 2014. Determination of the concentration of asbestos minerals in highly contaminated mine tailings: an example from abandoned mine waste of Crètaz and Èmarese (Valle d'Aosta, Italy). American Mineralogist, 99, 1233-1247.

Gunter, M.E., Belluso, E., Mottana, A., 2007. Amphiboles: Environmental and Health Concerns. Reviews in Mineralogy and Geochemistry, 67, 453-516.

Harper, M., 2008. 10th Anniversary Critical Review: Naturally Occurring Asbestos. Journal of Environmental Monitoring, 10, 1394-1408.

Health and Safety Executive, 2006. Asbestos: The analysts' guide for sampling, analysis and clearance procedures. Executive Health and Safety, ed. HSE Books, 120 pp.

Houchot, M.-A., 2008. De l'évaluation en santé publique à une démarche de géographie de la santé: le risque amiante environnemental en Nouvelle-Calédonie. Ph.D. thesis, Université de Nouvelle Calédonie, 282 pp.

IARC, 2012. Arsenic, Metals, Fibres, and Dusts. A review of human carcinogens. IARC Monographs on the Evaluation of Carcinogenic Risks to Humans, vol. 100C, Lyon, France, 501 pp.

IARC, 2017. Fluoro-edenite, silicon carbide fibres and whiskers, and single-walled and multi-walled carbon nanotubes. IARC Monographs on the Evaluation of Carcinogenic Risks to Humans, vol. 111, Lyon, France, 325 pp.

INSERM U88, 1997. Aspects épidémiologiques de la relation entre exposition environnementale à la trémolite et cancers respiratoires en Nouvelle-Calédonie. Saint-Maurice, 33 pp.

Jehlička, J., Vítek, P., Edwards, H.G.M., Heagraves, M., Čapoun, T., 2009. Application of portable Raman instruments for fast and non-destructive detection of minerals on outcrops. Spectrochimica Acta - Part A: Molecular and Biomolecular Spectroscopy, 73, 410-419.

Keeling, J.L., Raven, M.D., Self, P.G., Eggleton, R.A., 2008. Asbestiform antigorite occurrence in South Australia. In: 9th International Congress for Applied Mineralogy, ICAM 2008, Brisbane, Queensland, 329-336.

Keeling, J.L., Raven, M.D., Self, P.G., 2010. Asbestiform antigorite. Implications for the risk assessment of fibrous silicates. In: Extended Abstracts, 21st Australian Clay Minerals Conference, Brisbane, Queensland, 87-90.

Lagabrielle, Y., Chauvet, A., Ulrich, M., Guillot, S., 2013. Passive obduction and gravity-driven emplacement of large ophiolitic sheets: The New Caledonia ophiolite (SW Pacific) as a case study. Bulletin de la Societe Geologique de France, 184, 545-556.

Lahondère, D., 2007. L'amiante environnemental en Nouvelle Calédonie: expertise géologique des zones amiantifères. Evaluation des actions engagées. Nouméa, 55 pp.

Lahondère, D., 2012. Serpentinisation et fibrogenèse dans les massifs de péridotite de Nouvelle-Calédonie. Atlas des occurrences et des types de fibres d'amiante sur mine. Nouméa, 128 pp.

Laporte-Magoni, C., Tribaudino, M., Meyer, M., Fubini, B., Tomatis, M., Juillot, F., Petriglieri, J.R., Gunkel-Grillon, P., Selmaoui-Folcher, N., 2018. Amiante et Bonnes Pratiques. Rapport Final, Nouméa, Nouvelle Calédonie, 214 pp.

Lee, R.J., Strohmeier, B.R., Bunker, K.L., Van Orden, D.R., 2008. Naturally Occurring Asbestos - A recurring public policy challenge. Journal of Hazardous Materials, 153, 1-21.

Leguere, J., 1976. Des correlations entre la tectonique cassante et l'alteration supergene des peridotites de Nouvelle Caledonie. Ph.D. thesis, Université de Montpellier, 95 pp.

Luce, D., Brochard, P., Quenel, P., Salomon-Nekiriai, C., Goldberg, P., Billon-Galland, M.-A., Goldberg, M., 1994. Malignant pleural Mesothelioma associated with exposure to tremolite. The Lancet, 344, 1777.

Luce, D., Bugel, I., Goldberg, P., Goldberg, M., Salomon, C., Billon-Galland, M.-A., Nicolau, J., Quénel, P., Fevotte, J., Brochard, P., 2000. Environmental exposure to tremolite and respiratory cancer in New Caledonia: a case-control study. American Journal of Epidemiology, 151, 259-265.

Luce, D., Billon-Galland, M.-A., Bugel, I., Goldberg, P., Salomon, C., Févotte, J., Goldberg, M., 2004. Assessment of environmental and domestic exposure to tremolite in New Caledonia. Archives of Environmental Health, 59, 91-100.

Mothersole, F.E., Evans, K.A., Frost, B.R., 2017. Abyssal and hydrated mantle wedge serpentinised peridotites: a comparison of the 15°20′N fracture zone and New Caledonia serpentinites. Contributions to Mineralogy and Petrology, 172, 1-25.

Musa, M., Croce, A., Allegrina, M., Rinaudo, C., Belluso, E., Bellis, D., Toffalorio, F., Veronesi, G., 2012. The use of Raman spectroscopy to identify inorganic phases in iatrogenic pathological lesions of patients with malignant pleural mesothelioma. Vibrational Spectroscopy, 61, 66-71.

NF X 43-269. Mars 2002 Qualité de l'air - Air des lieux de travail - Détermination de la concentration en nombre de fibres par microscopie optique en contraste de phase - Méthode du filtre à membrane. AFNOR (Indice de classement: X43-269).

Nichols, M.D., Young, D., Gray, D., 2002. Guidelines for geologic investigations of Naturally Occurring Asbestos in California. California Geological Survey, Special Publication 124, 85 pp.

Noonan, C.W., 2017. Environmental asbestos exposure and risk of mesothelioma. Annals of Translational Medicine, 5, 234-234.

Orloff, O., Gonord, H., 1968. Note préliminaire sur un nouveau complexe sédimentaire continental situé sur les massifs du Goa N'Doro et de Kadjitra (région côtière à l'Est de la Nouvelle-Calédonie), définition de la formation et conséquences de cette découverte sur l'âge des fractures. Comptes Rendus de l'Académie des Sciences, 267, 5-8.

Petriglieri, J.R., Salvioli-Mariani, E., Mantovani, L., Tribaudino, M., Lottici, P.P., Laporte-Magoni, C., Bersani, D., 2015. Micro-Raman mapping of the polymorphs of serpentine. Journal of Raman Spectroscopy, 46, 953-958.

Petry, R., Mastalerz, R., Zahn, S., Mayerhöfer, T.G., Völksch, G., Viereck-Götte, L., Kreher-Hartmann, B., Holz, L., Lankers, M., Popp, J., 2006. Asbestos mineral analysis by UV Raman and energy-dispersive X-ray spectroscopy. ChemPhysChem, 7, 414-420.

Prinzhofer, A., 1981. Structure et pétrologie d'un cortège ophiolitique: Le massif du sud (Nouvelle Calédonie). Ph.D. thesis, Ecole Nationale Supérieure des Mines, Paris, 185 pp.

Quesnel, B., 2015. Alteration supergene, circulation des fluides et deformation interne du mas- sif de Koniambo, Nouvelle-Caledonie: implication sur les gisements nickeliferes lateritiques. Ph.D. thesis, Université de Rennes 1, 316 pp.

Quesnel, B., Gautier, P., Cathelineau, M., Boulvais, P., Couteau, C., Drouillet, M., 2016. The internal deformation of the Peridotite Nappe of New Caledonia: A structural study of serpentine-bearing faults and shear zones in the Koniambo Massif. Journal of Structural Geology, 85, 51-67.

Rawling, T.J., Lister, G.S., 1999. Oscillating modes of orogeny in the Southwest Pacific and the tectonic evolution of New Caledonia. Geological Society, London, Special Publications, 154, 109-127.

Rinaudo, C., Gastaldi, D., Belluso, E., 2003. Characterization of chrysotile, antigorite, and lizardite by FT-Raman Spectroscopy. The Canadian Mineralogist, 41, 883-890.

Rinaudo, C., Gastaldi, D., Belluso, E., Capella, S., 2005. Application of Raman spectroscopy on asbestos fibre identification. Neues Jahrbuch Fur Mineralogie-Abhandlungen, 182, 31-36.

Rooney, J.S., Tarling, M.S., Smith, S.A.F., Gordon, K.C., 2018. Submicron Raman spectroscopy mapping of serpentinite fault rocks. Journal of Raman Spectroscopy, 49, 279-286.

Schreier, H., 1989. Asbestos fibres in the soil environment. In: Asbestos in the natural environment, first ed. Elsevier, vol. 37, 68-94.

Tarling, M.S., Rooney, J.S., Viti, C., Smith, S.A.F., Gordon, K.C., 2018. Distinguishing the Raman spectrum of polygonal serpentine. Journal of Raman Spectroscopy, 1-7.

Thompson, B.D., Gunter, M.E., Wilson, M.A., 2011. Amphibole asbestos soil contamination in the USA: a matter of definition. American Mineralogist, 96, 690-693.

Tomatis, M., Gazzano, E., Aldieri, E., Turci, F., Fubini, B., Laporte-magoni, C., 2018. Potential toxicity of fibrous antigorite from New Caledonia: variability and similarities with chrysotile asbestos. In: XXII Meeting of the International Mineralogical Association, Melbourne, Australia, 457.

Trescases, J.-J., 1975. Supergenic geochemical evolution of the ultrabasic rocks in the tropical zone-formation of the nickeliferous deposits in New Caledonia. Memoires, ORSTOM ed., Paris, 259 pp.

Trotet, F., 2012. Fibrous serpentinites in oxyded nickel ores from New Caledonia: risk management in a modern mining company - societal implications. In: 3rd Serpentine Days, Porquerolles Island, France, 87.

Trotet, F., Kadar, M., Marini, D., 2015. Typology of the New Caledonian Ni-laterite deposits: from natural to industrial processes. In: The Society for Geology Applied to Mineral Deposits, 13th SGA meeting.

Turci, F., Tomatis, M., Gazzano, E., Riganti, C., Martra, G., Bosia, A., Ghigo, D., Fubini, B., 2005. Potential toxicity of nonregulated asbestiform minerals: Balangeroite from the Western Alps. Part 2: oxidant activity of the fibres. Journal of Toxicology and Environmental Health, Part A, 68, 21-39.

Ulrich, M., 2010. Péridotites et serpentinites du complexe ophiolitique de la Nouvelle-Calédonie. Études pétrologiques, géochimiques et minéralogiques sur l'évolution d'une ophiolite de sa formation à son altération. Ph.D. thesis. Université de la Nouvelle-Caledonie and Université Joseph Fourier de Grenoble.

Ulrich, M., Picard, C., Guillot, S., Chauvel, C., Cluzel, D., Meffre, S., 2010. Multiple melting stages and refertilization as indicators for ridge to subduction formation: The New Caledonia ophiolite. Lithos, 115, 223-236.

Vignaroli, G., Ballirano, P., Belardi, G., Rossetti, F. 2014. Asbestos fibre identification vs. evaluation of asbestos hazard in ophiolitic rock mélanges, a case study from the Ligurian Alps (Italy). Environmental Earth Sciences, 72, 3679-3698.

Wacaster, S., 2011. The mineral industry of New Caledonia. U.S. Department of the Interior, Geological Survey, 8 pp.

Wagner, J., 2015. Analysis of serpentine polymorphs in investigations of Natural Occurrences of Asbestos. Environmental science, processes & impacts, 17, 985-96.

WHO, 1997. Determination of airborne fibre number concentrations. A recommended method, by phase-contrast optical microscopy (membrane filter method). World Health Organization, Geneva, 61 pp.

Wicks, F.J., Whittaker, E.J.W., 1977. Serpentine Texture and Serpentinization. Canadian Mineralogist, 15, 459-488.

Figure captions

Figure 1. Geological sketch map of the ultramafic allochthon of New Caledonia (redrawn and modified after Cluzel et al., 2001). Potentially NOA are reported (DIMENC-SGNC, 2010). Sampling sites of Tontouta and Poro mines are indicated with star.

Figure 2. Fibrous-lamellar antigorite showing several degrees of alteration on the outcrop, Koniambo massif, New Caledonia (from Mission XTRATA Amiante 2012).

Figure 3. Macroscopic features of Caledonian samples. An evident lack of coherence and a very altered appearance occur.

Figure 4. Raman spectra of altered tremolite (Sample 36, Poro mine, NC) recorded by Raport handheld instrument (532-nm laser).

Figure 5. Raman spectra of fibrous antigorite (Tontouta mine, NC) recorded by Raport handheld instrument (532-nm laser) and by laboratory Raman microspectrometer (473-nm laser), including the region of the OH stretching vibrations.

Figure 6. Discrimination of antigorite from chrysotile fibres by PLM/DS. Chrysotile (Sample 57), RI 1.550: a) Phase Contrast: pale-blue, with orange halo; b) Dark Field: blue/purple. Antigorite (Sample 6), RI 1.5680: c) Phase Contrast: pale-blue to white, no halo; d) Dark Field: blue/blue indigo.

Figure 7. Identification of tremolite by PLM/DS, RI 1.605. Phase Contrast: pale-blue to dark-grey, orange halo; Dark Field: yellow to purple. Sample 36.

Figure 8. Identification of sample 33. a) stereomicroscope observation: parallel welded lamellae; b) PLM/DS, RI 1.550: pale-blue, with orange halo; c) Raman spectrum of chrysotile (Raport handheld instrument, 532-nm laser); d) SEM image showing a compact bundle of parallel chrysotile fibrils.

Figure 9. Identification of sample 33 by TEM-SAED. a) TEM micrograph showing a group of well separated fibre with larger inner-channel and variable aspect ratio; b) SAED of a single fibril of clino-chrysotile.

Figure 10. Investigation of intimately intergrowth (cross-polarizing and SEI images) of chrysotile fibres (a) and fibrous-lamellar antigorite (b) by means of micro-Raman spectroscopy. Raman spectra were obtained at 473.1 nm in the high-wavenumber region. Sample 30.

Figure 11. SEM image of antigorite. Several breathable fibrous-lamellae occur at the surface. Sample 13.

Table caption

Table 1. List of the eight most representative selected samples out of fifty investigated rock-fragments. In the table are also reported results obtained by visual on-field versus analytical investigation.

Table 2. Mineralogical identification of selected samples. *In situ* monitoring versus laboratory investigation have been compared.

Supplementary Items

Table A. Sampling report. List of investigated rock fragments, together with provenance and alteration status. Results obtained by visual on-field versus analytical identification are reported.

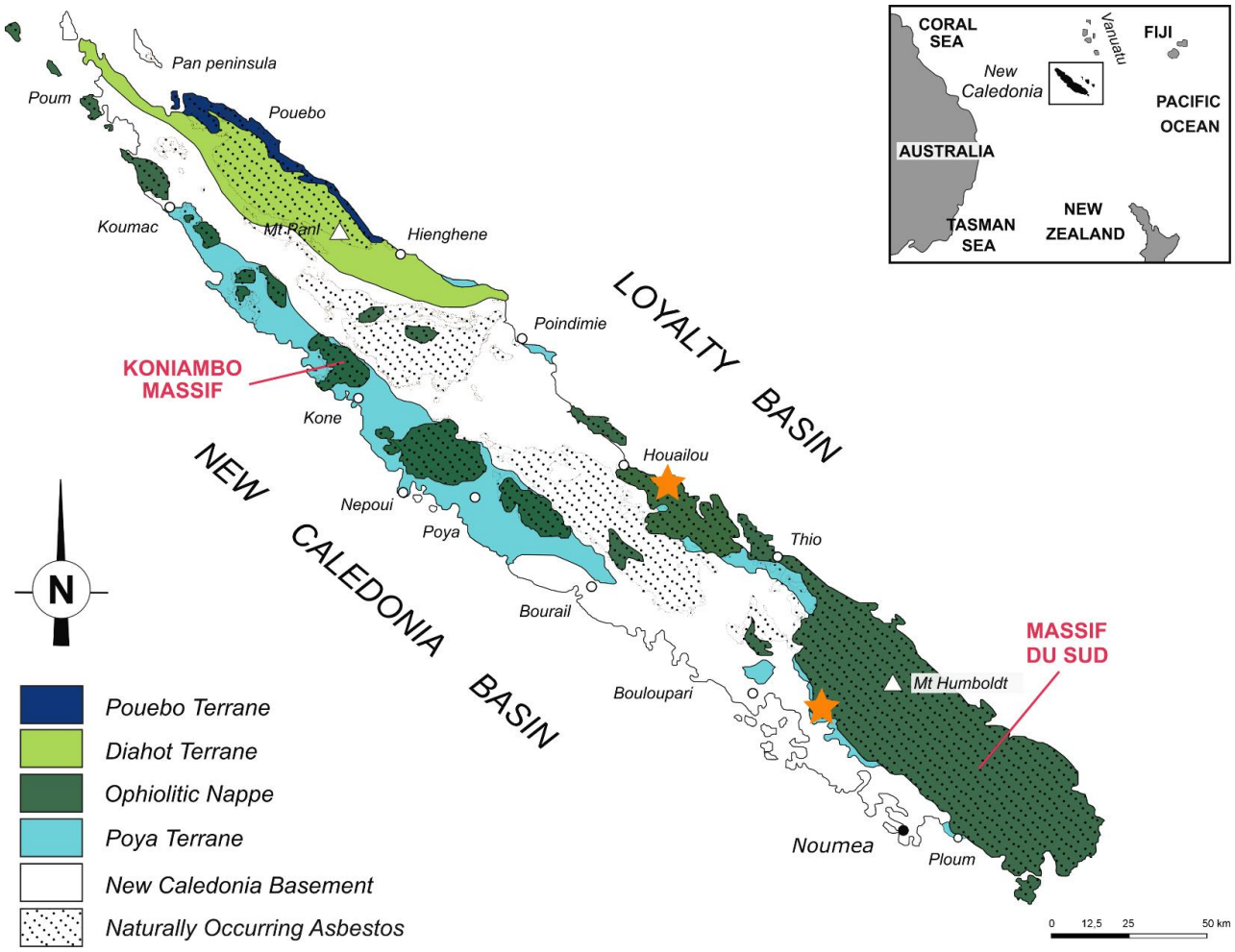

Figure 1. Geological sketch map of the ultramafic allochthon of New Caledonia (redrawn and modified after Cluzel et al., 2001). Potentially NOA are reported (DIMENC-SGNC, 2010). Sampling sites of Tontouta and Poro mines are indicated with star.

Figure 2. Fibrous-lamellar antigorite showing several degrees of alteration on the outcrop, Koniambo massif, New Caledonia (from Mission XTRATA Amiante 2012).

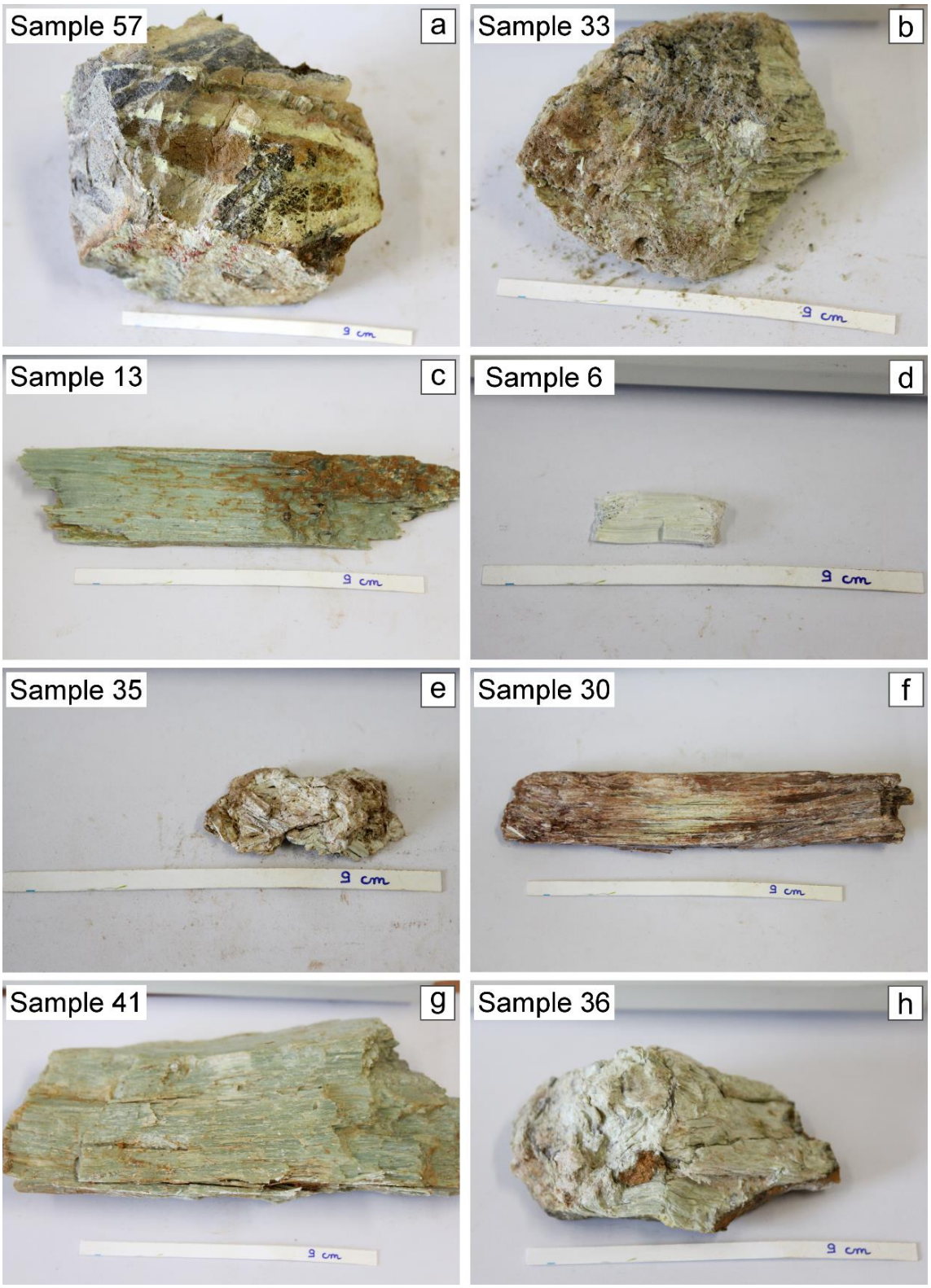

Figure 3. Macroscopic features of Caledonian samples. An evident lack of coherence and a very altered appearance occur.

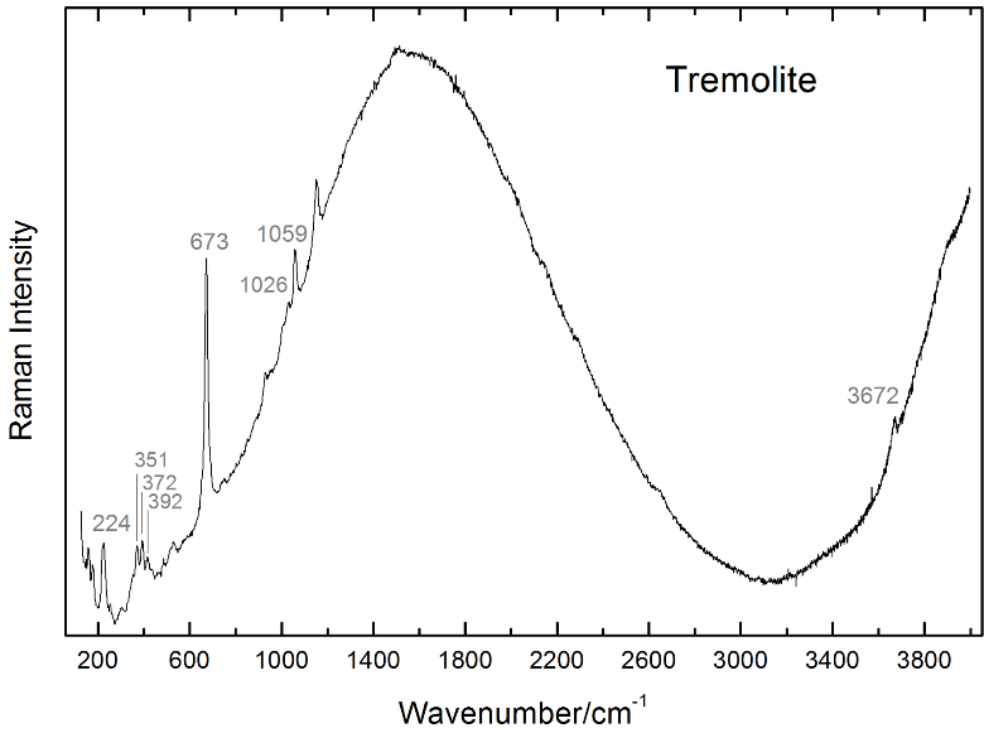

Figure 4. Raman spectra of altered tremolite (Sample 36, Poro mine, NC) recorded by Raport handheld instrument (532-nm laser).

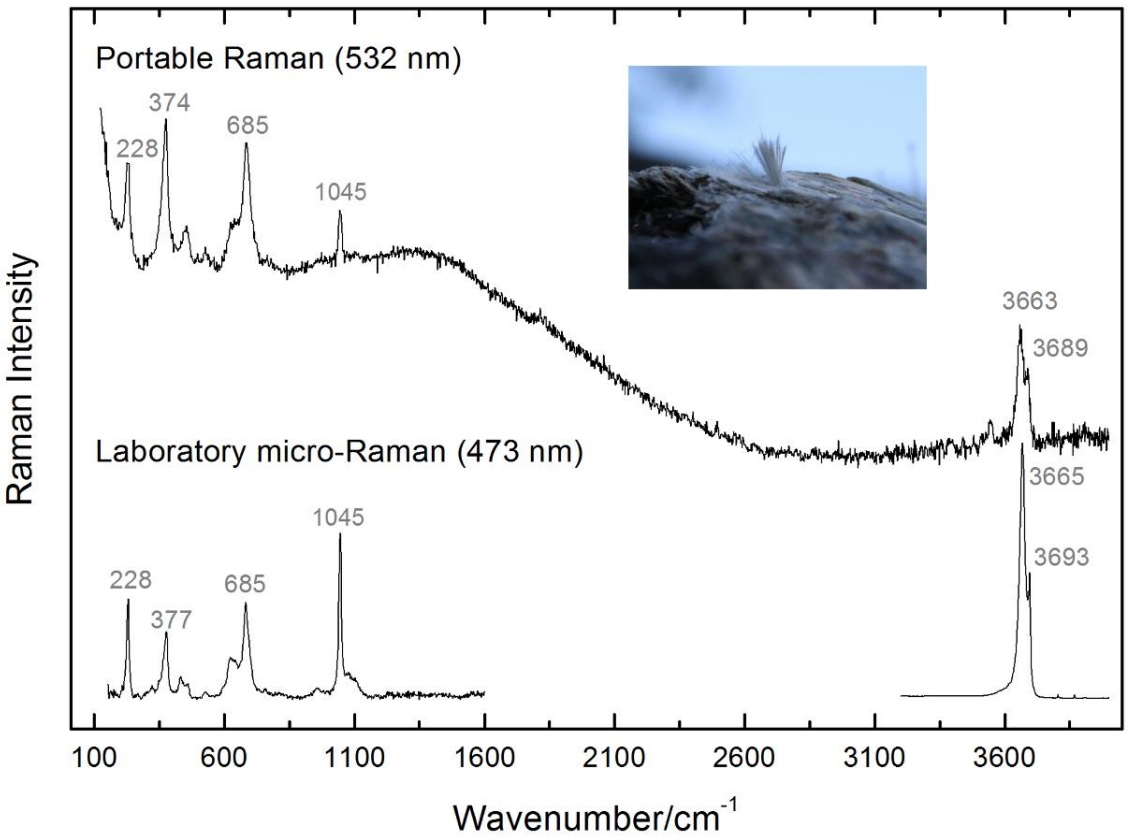

Figure 5. Raman spectra of fibrous antigorite (Tontouta mine, NC) recorded by Raport handheld instrument (532-nm laser) and by laboratory Raman microspectrometer (473-nm laser), including the region of the OH stretching vibrations.

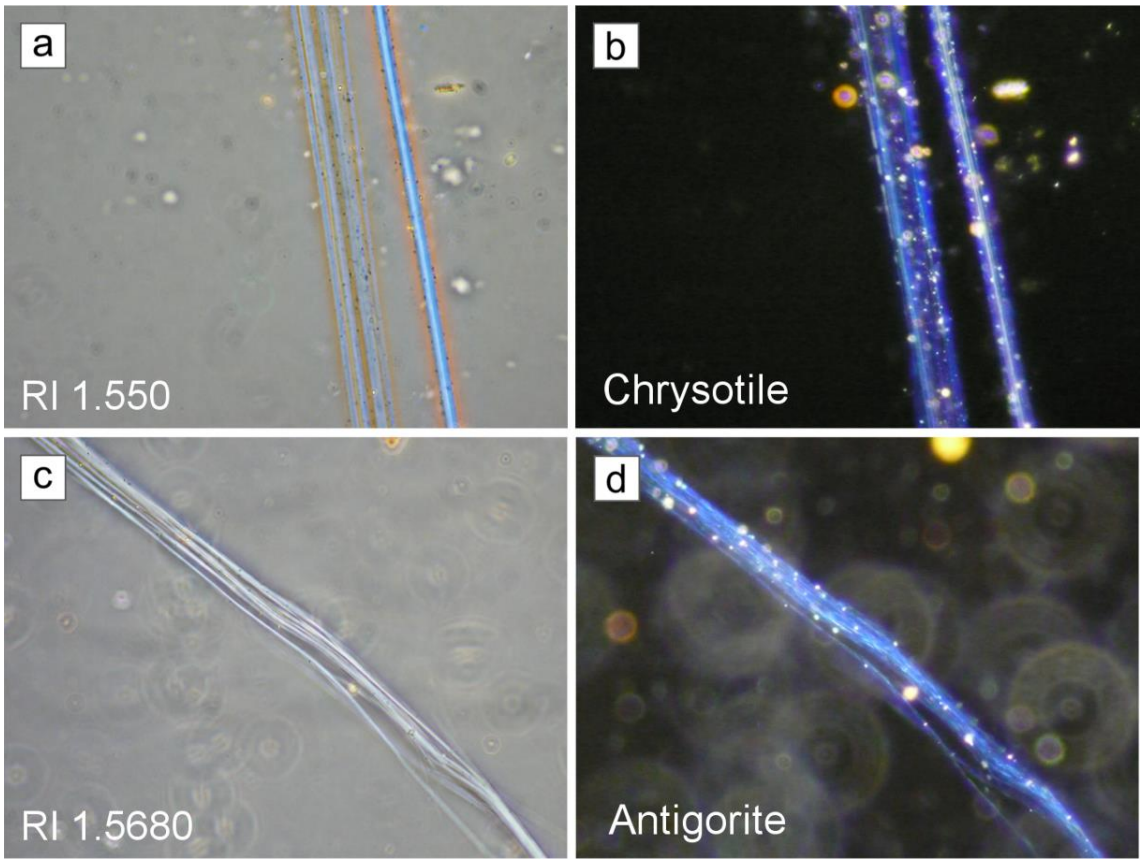

Figure 6. Discrimination of antigorite from chrysotile fibres by PLM/DS. Chrysotile (Sample 57), RI 1.550: a) Phase Contrast: pale-blue, with orange halo; b) Dark Field: blue/purple. Antigorite (Sample 6), RI 1.5680: c) Phase Contrast: pale-blue to white, no halo; d) Dark Field: blue/blue indigo.

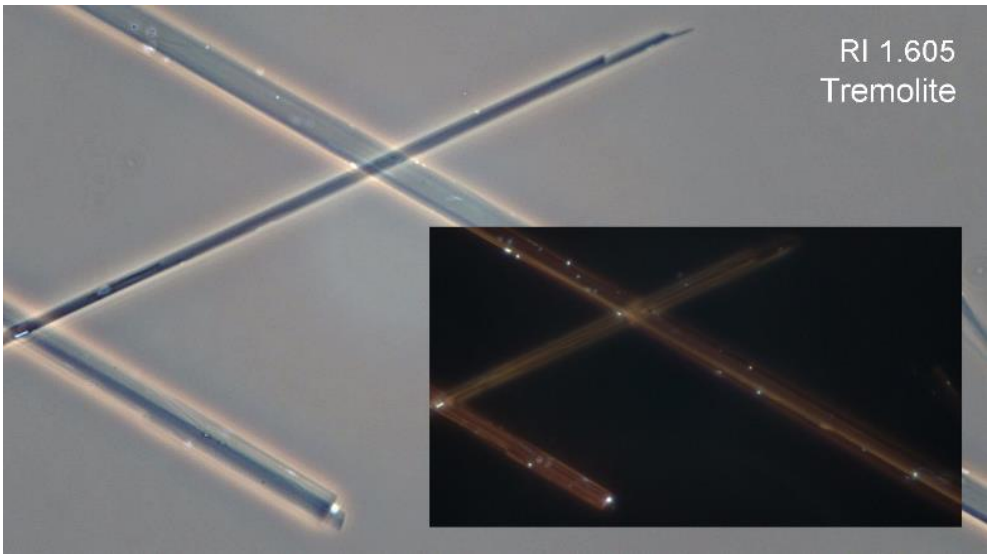

Figure 7. Identification of tremolite by PLM/DS, RI 1.605. Phase Contrast: pale-blue to dark-grey, orange halo; Dark Field: yellow to purple. Sample 36.

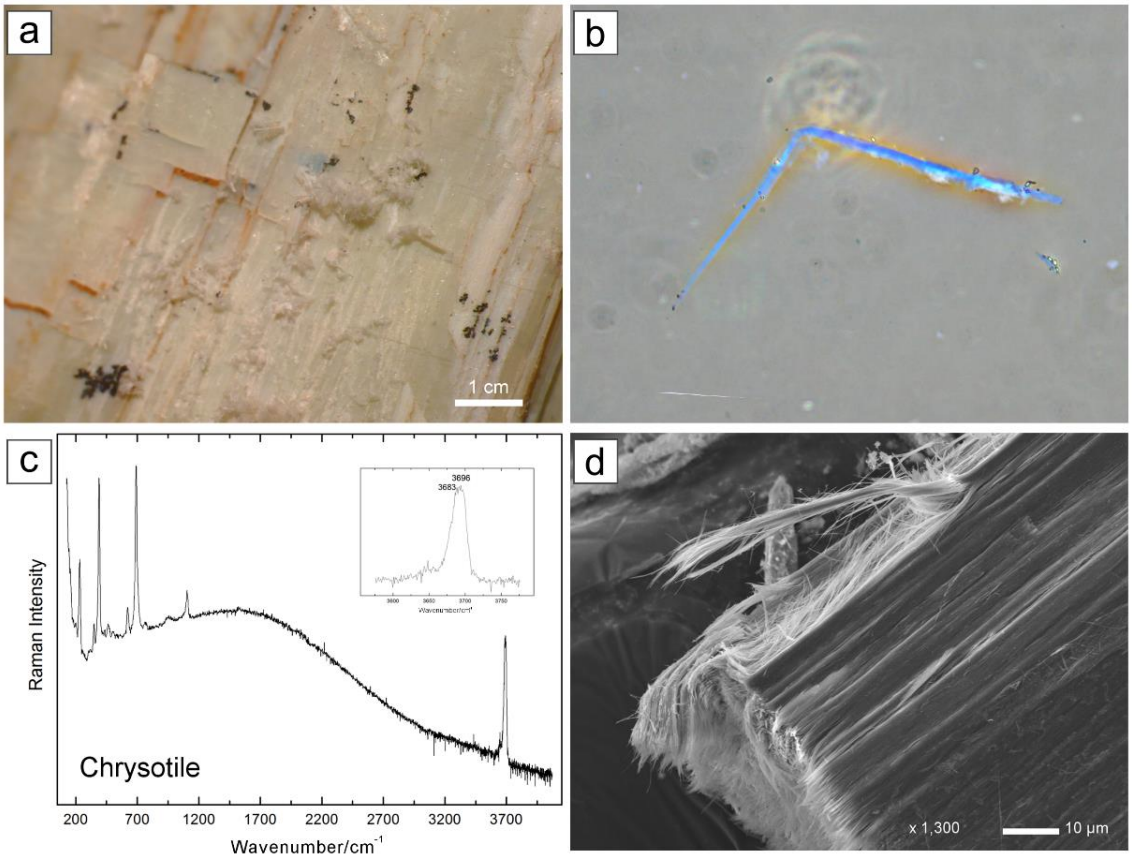

Figure 8. Identification of sample 33. a) stereomicroscope observation: parallel welded lamellae; b) PLM/DS, RI 1.550: pale-blue, with orange halo; c) Raman spectrum of chrysotile (Raport handheld instrument, 532-nm laser); d) SEM image showing a compact bundle of parallel chrysotile fibrils.

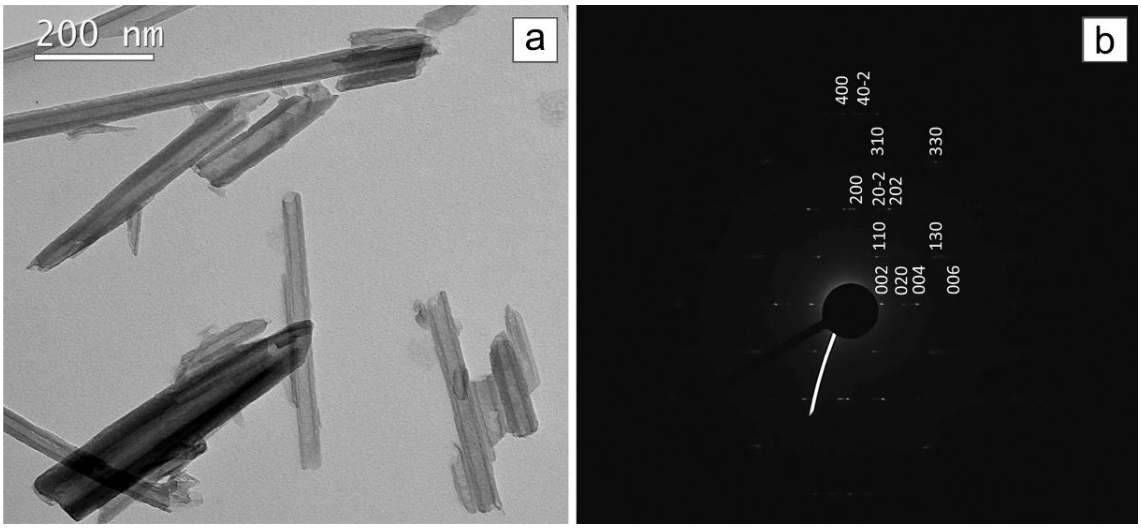

Figure 9. Identification of sample 33 by TEM-SAED. a) TEM micrograph showing a group of well separated fibre with larger inner-channel and variable aspect ratio; b) SAED of a single fibril of clino-chrysotile.

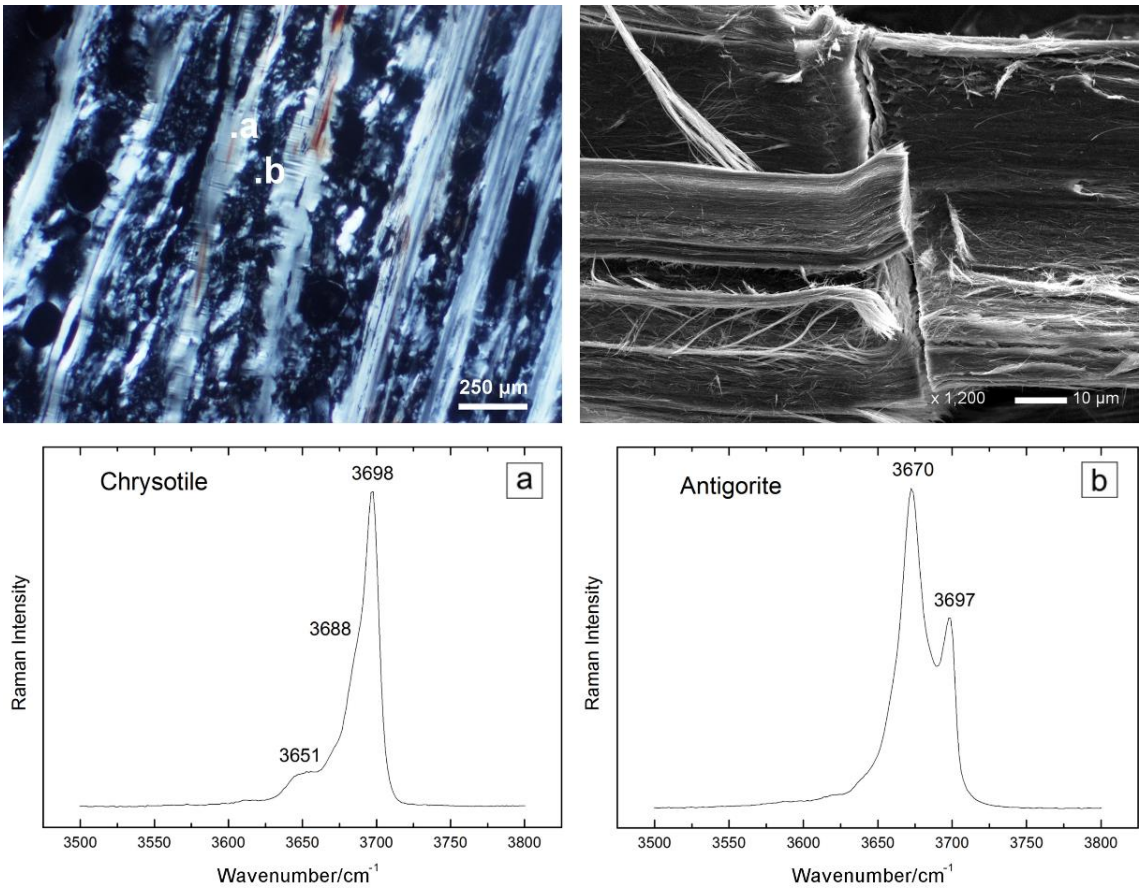

Figure 10. Investigation of intimately intergrowth (cross-polarizing and SEI images) of chrysotile fibres (a) and fibrous-lamellar antigorite (b) by means of micro-Raman spectroscopy. Raman spectra were obtained at 473.1 nm in the high-wavenumber region. Sample 30.

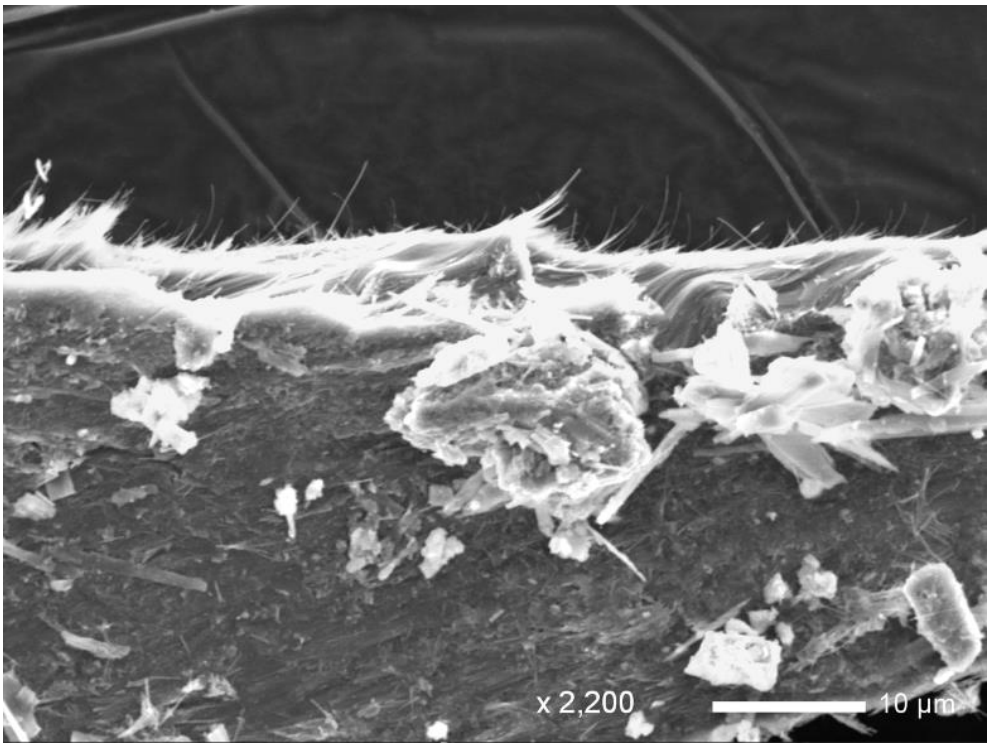

Figure 11. SEM image of antigorite. Several breathable fibrous-lamellae occur at the surface. Sample 13.

	Provenance / Mine site	Alteration status	On field identification	Analytical identification
Sample 41	Poro	non-altered	Tremolite	Tremolite & Serpentine
Sample 36	Poro	high-altered	Tremolite	Tremolite & Serpentine
Sample 57	Poro	-	Chrysotile	Chrysotile
Sample 33	Tontouta	non-altered	Antigorite	Chrysotile
Sample 13	Tontouta	non-altered	Antigorite	Antigorite
Sample 6	Tontouta	medium-altered	Antigorite	Antigorite
Sample 35	Tontouta	high-altered	Antigorite	Antigorite
Sample 30	Tontouta	non-altered	Antigorite	Antigorite & Chrysotile

Table 1. List of the eight most representative selected samples out of fifty investigated rock-fragments. In the table are also reported results obtained by visual on-field versus analytical investigation.

	On field geological survey	Laboratory investigation				*In situ* identification	
		PLM (thin section)	SEM/EDS	TEM/SAED	micro-Raman	PLM/DS (mount particles)	Portable Raman
Sample 41	Tremolite	Tremolite & Serpentine	Tremolite & Serpentine	-	-	RI.1605 Tremolite	Tremolite
Sample 36	Tremolite	Tremolite & Serpentine	Tremolite & Serpentine	-	-	RI.1605 Tremolite	Tremolite
Sample 57	Chrysotile	Chrysotile	Chrysotile	Chrysotile	Chrysotile	RI. 1550 Chrysotile	Chrysotile
Sample 33	Antigorite	Chrysotile	Chrysotile	Chrysotile	Chrysotile	RI. 1550 Chrysotile	Chrysotile
Sample 13	Antigorite	Lamellar serpentine (Antigorite)	Antigorite	-	Antigorite	RI 1.5680 Antigorite	Antigorite
Sample 6	Antigorite	Serpentine (Antigorite)	Fibrous-lamellar Antigorite	-	Antigorite	RI 1.5680 Antigorite	Antigorite
Sample 35	Antigorite	Serpentine (Antigorite)	Fibrous Antigorite	-	Antigorite	RI 1.5680 (fibrous) Antigorite	Antigorite
Sample 30	Antigorite	Antigorite & Chrysotile	Fibrous serpentine	-	Antigorite & Chrysotile	RI 1.550 & 1.5680 Chrysotile & Antigorite	Antigorite & Chrysotile

Table 2. Mineralogical identification of selected samples. *In situ* monitoring versus laboratory investigation have been compared.